

Fig. 1 Norm of tracking error e and the effects of air drag and gravity.

amount of acceleration has been used to denote the required energy consumption for the landing process.^{1,3,4} In this study, we adopt the same idea to employ the norm of the control input u for expressing the required energy for landing. The relationship between control effort and mass of propellant m_p required for landing can be expressed as¹¹ $\int \|u\| dt \propto \ln[m_0/(m_0 - m_p)]$, where m_0 is the initial vehicle mass.

Conclusion

We have considered the rendezvous of a space vehicle with a celestial object. The study included the effects of drag and disturbance. By employing the variable structure control technique, a continuous guidance law has been proposed to guarantee the tracking performance and alleviate the classical chattering drawback. The tracking performance has the property of exponential convergence rate, which can be assigned by the designer. Finally, an illustrative example was presented to demonstrate the use of the main results.

Acknowledgment

This research was supported by the National Science Council, Taiwan, Republic of China under Grant NSC 88-2212-E-009-022.

References

- Yuan, P. J., and Hsu, S. C., "Rendezvous Guidance with Proportional Navigation," *Journal of Guidance, Control, and Dynamics*, Vol. 17, No. 2, 1993, pp. 409–411.
- Shaohua, Y., "Terminal Spacecraft Coplanar Rendezvous Control," *Journal of Guidance, Control, and Dynamics*, Vol. 18, No. 4, 1995, pp. 838–842.
- Guelman, M., "Guidance for Asteroid Rendezvous," *Journal of Guidance, Control, and Dynamics*, Vol. 14, No. 5, 1991, pp. 1080–1083.
- Guelman, M., and Harel, D., "Power Limited Soft Landing on an Asteroid," *Journal of Guidance, Control, and Dynamics*, Vol. 17, No. 1, 1994, pp. 15–20.
- Robert, N. I., "Guidance and Control System Design of the Viking Planetary Lander," *Journal of Guidance, Control, and Dynamics*, Vol. 1, No. 3, 1978, pp. 189–196.
- Lafontaine, J. D., "Autonomous Spacecraft Navigation and Control for Comet Landing," *Journal of Guidance, Control, and Dynamics*, Vol. 15, No. 3, 1992, pp. 567–576.
- Myint-U, T., "Effect of Oblateness and Drag on Equatorial Orbits with Small Eccentricities," *Journal of Spacecraft and Rockets*, Vol. 5, No. 1, 1968, pp. 123–125.
- Wertz, J. R., and Larson, W. J., *Space Mission Analysis and Design*, Kluwer Academic, Norwell, MA, 1991, Chap. 6, pp. 123–129.
- Yang, C. D., and Yang, C. C., "Analytical Solution of Three-Dimensional Realistic True Proportional Navigation," *Journal of Guidance, Control, and Dynamics*, Vol. 19, No. 3, 1996, pp. 569–577.
- Persen, L. N., "Motion of a Satellite with Friction," *Jet Propulsion*, Vol. 28, No. 11, 1958, pp. 750–752.
- Das, B. M., Kassimali, A., and Sami, S., *Engineering Mechanics: Dynamics*, Richard D. Irwin, 1994, Chap. 5, pp. 217–221.

Setpoint Generation for Constant-Velocity Motion of Space-Based Scanners

Rebecca A. Masterson*

Massachusetts Institute of Technology,
Cambridge, Massachusetts 02139

William E. Singhose†

Georgia Institute of Technology, Atlanta, Georgia 30332
and

Warren P. Seering‡

Massachusetts Institute of Technology,
Cambridge, Massachusetts 02139

I. Introduction

THE performance of flexible spacecraft that contain constant-velocity scanning payloads is degraded by vibration that corrupts the desired motion. The vibration disturbances can come from numerous sources including gravity gradients, attitude control reaction wheels,^{1–3} jet propulsion systems,^{4–6} thermoelastic deformation,^{7,8} fluid sloshing,⁹ and payload-payload interactions.¹⁰ There are a number of possible ways to deal with these corrupting disturbances such as using vibration isolation systems,¹¹ concurrently designing the structure and controller,¹² and generating vibration-reducing motion setpoints.¹³ Scanners often need to perform rapid changes in velocity and direction to achieve high cycle throughput. These setpoint changes can induce vibration that corrupts the constant-velocity portion of the scanning cycle. In this case, the scanner motion corrupts its own signal.

Consider the position profile shown in Fig. 1. The profile has several regions where the desired scanning velocity is constant ($\pm v_1$). These constant-velocity regions are separated by high-velocity regions ($\pm v_2$) and changes in direction. This type of command is used with systems that perform constant-velocity scanning over sub regions of their workspace. Between these regions, the system attempts to move rapidly to the next scanning region. If the system has flexibility, then the response will contain vibration superimposed on the constant-velocity motion.

Regions 1–4 of Fig. 1 represent the position ranges over which the mass is required to move at the constant velocity, v_1 , while performing the scanning operation. An auxiliary goal is to move the system as slowly as possible over the scan regions while keeping the total duration of the cycle fixed. The slow scanning velocity allows the sensor more time to make a measurement and, consequently, the accuracy is improved.

The profile shown in Fig. 1 was chosen because it is representative of high-performance scanning profiles. There is much to gain by using high-velocity motions between the scanning regions. If the system traveled at a single constant velocity over both the scanning and nonscanning regions, the slowest scan velocity it could use (given the position set points in Fig. 1) while still completing a cycle in the desired time (0.25 s in this example) would be 6.24 cm/s. However, if the nonscan velocity v_2 were infinite, the system could traverse the scanning regions as slowly as 2.4 cm/s while still completing the cycle in 0.25 s.

The ideal profile, then, has the smallest possible scanning velocity v_1 and infinite nonscanning velocity v_2 . This profile allots the maximum time available for the scanning process. The time available for

Received 14 June 1999; revision received 25 April 2000; accepted for publication 26 April 2000. Copyright © 2000 by the American Institute of Aeronautics and Astronautics, Inc. All rights reserved.

*Research Assistant, Department of Mechanical Engineering, Member AIAA.

†Assistant Professor, Department of Mechanical Engineering, Member AIAA.

‡Professor, Department of Mechanical Engineering.

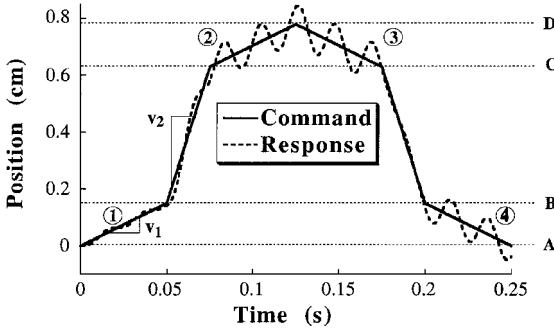


Fig. 1 Benchmark command and system response.

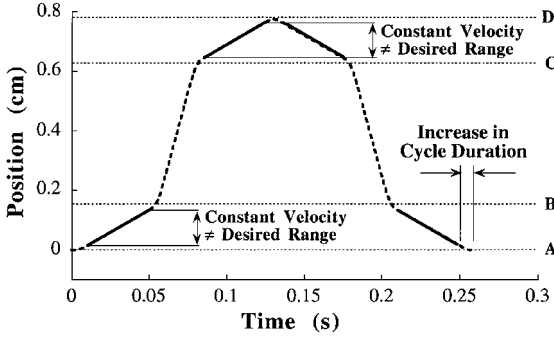


Fig. 2 ZV shaped position response.

scanning, t_1 , can be found using the cycle duration constraint and the simple relationship between time and velocity:

$$t_1 = \frac{1}{2}[L_{\text{com}}/2 - (C - B)/v_2] \quad (1)$$

where L_{com} is the cycle duration and C and B are the position points shown in Fig. 1. This equation shows that the time available for scanning increases with nonscanning velocity.

Given the cycle duration constraint, t_1 cannot be larger than one fourth of the total cycle time (there are four scan regions per cycle), then in order to achieve the maximum t_1 , v_2 must be infinite. However, it can be shown using Eq. (1) that t_1 reaches 90% of its maximum value at a relatively low nonscanning velocity. Therefore, little is gained by setting v_2 to an unreasonably high value. The input profile shown in Fig. 1 has a scan velocity of 3 cm/s. This profile requires v_2 to have a value of 19.2 cm/s to complete the cycle in 0.25 s.

The response to the scanning profile of an undamped second-order system with a frequency of 50 Hz is shown in Fig. 1. Note that the vibration causes the velocity to vary considerably during the scanning regions. The process of input shaping¹³ can be used to reduce the vibration from the setpoint changes; however, additional problems are introduced. Input shaping is a command generation scheme that generates reference commands that are self-canceling. Any vibration induced by the command is canceled by a later portion of the command. Input shaping is implemented by convolving the reference command with a special sequence of impulses. The convolution product is then used as the new reference command. This Note presents a setpoint generation scheme, based on input shaping, that produces low levels of vibration during the constant-velocity portion of a scanning cycle.

II. Effect of Input Shaping

The detrimental effects of flexibility on system performance are obvious from Fig. 1. In this section input shaping is used to eliminate the vibration. It will be shown that input shaping distorts the length of the scanning regions. Section III will present a method to alter the unshaped command and produce results that better track the desired profile.

The command profile of Fig. 1 was convolved with a Zero-Vibration (ZV) shaper^{13,14} to produce a command that removes the residual vibration from the response. The response to the shaped command is shown in Fig. 2. The improvement that results from

input shaping is quite obvious. However, note that the shaped command duration is longer than the original command duration and that the corners of the velocity profile have become slightly rounded. The shaped command is longer than the unshaped command by the duration of the input shaper. The duration of a ZV shaper is equal to $T/2$, where T is the period of the system vibration. Therefore, changes in the command profile will not take place instantaneously but over a time duration of $T/2$ s. The dotted horizontal lines labeled A, B, C, and D in Fig. 2 indicate the beginning and end of the desired constant-velocity regions. Note that although the shaped response does not vibrate, it does not follow the desired position profile exactly. Changes from one velocity to another take longer to occur, thereby shortening the constant-velocity scan regions.

III. Augmenting the Input Shaping Process

To make input shaping more advantageous for this type of system, the discrepancies between the desired and actual scanning regions must be reduced. This goal can be achieved by modifying the unshaped command in such a way that the shaped command is at constant velocity for the desired position ranges.

As previously noted, the duration of the shaped response exceeds the desired cycle time by the duration of the shaper L_{shap} . This problem can be easily solved by shortening the length of the unshaped command. The new unshaped command length L_{new} is

$$L_{\text{new}} = L_{\text{com}} - L_{\text{shap}} \quad (2)$$

Solving the problem of the shortened scan regions is more involved. It is possible to lengthen these regions of the unshaped command by a distance d at both ends. This distance is found by assuming the velocity in the nonscanning regions is set to a maximum. Then, using the definition of velocity and dividing by 2 to distribute the distance at both ends of the scanning regions

$$d = v_1 L_{\text{shap}}/2 \quad (3)$$

When the modified command is convolved with an input shaper, the shaped command will be at constant velocity over the desired scanning ranges. The extra distance d , will accommodate the time the shaped command takes to ramp up to the scanning velocity. However, the command will be longer than the desired command because additional time is required to traverse the additional distance. Therefore, the velocity in the scan regions must be increased to shorten the cycle time back to the desired value, while holding v_2 at its maximum possible value (19.2 cm/s in the example problem considered here). This new scanning velocity is then used to calculate a new value of d . The difference between the new d and the original d is added to both ends of the scan regions, and the scan velocity is again increased. This iterative process continues until the difference between the new d and the one previous is negligible, that is,

$$|d_{n-1} - d_n| < \delta \quad (4)$$

where n is the total number of iterations performed. Figure 3 shows the position response of the system to the modified command shaped with a ZV shaper. The areas of constant velocity now extend over the entire desired scanning regions. Using the modified command,

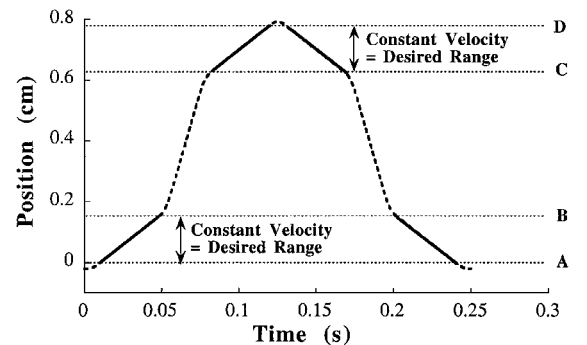


Fig. 3 Position response to modified ZV shaped command.

the position response closely follows the desired position profile with no velocity oscillation.

Although ZV shaping, along with modification of the original command, greatly improves system performance, it does have one drawback. To modify the command to accommodate the shaper length, the scan regions are lengthened, and the scan velocity must be increased to keep the total cycle duration constant. However, as mentioned previously, for good performance, a scanning system often requires a low scanning velocity. In this respect, ZV shaping actually degrades the performance of the system. One way to lower v_1 is to use an input shaper with a shorter duration, such as those containing negative impulses. If negative impulses are used, then their magnitudes must be limited in some way to avoid actuator saturation. One good way of doing this is to limit the impulse amplitudes to ± 1 . Shapers created with these amplitude values are called Unity-Magnitude (UM) shapers.¹⁵ The UM ZV shaper has a duration of only $T/3$, as compared to the positive ZV shaper whose amplitude is $T/2$.

ZV shapers are sensitive to modeling errors: small modeling errors may lead to significant vibration. Therefore, the velocity response of this system could vary considerably with small changes in the plant dynamics. This fact may require the use of the robust input shapers. One type of robust shaper can be obtained by requiring the derivative of the vibration, with respect to the frequency, to be zero at the modeling frequency. These types of shapers are called Zero Vibration and Derivative (ZVD) shapers.¹³ They have the effect of keeping the vibration near zero even when there is a significant error in the estimation of the system frequency. This property can be visualized by plotting the amplitude of vibration vs the modeling error. Such a sensitivity curve is shown in Fig. 4. To measure the robustness quantitatively, one can measure the width of the sensitivity curve that is below a tolerance threshold. This width is called the shaper's insensitivity. The 5% insensitivity has been labeled on Fig. 4.

Figure 5 shows the velocity responses to ZV, UM ZV, ZVD, and UM ZVD shaped commands. Note that the scan velocity with the UM ZV shaper is lower than that with the ZV shaper. Similarly, the scanning velocity with the UM ZVD shaper is significantly lower than with the ZVD shaper, but it is somewhat higher than the scanning velocity of the ZV shaper. A quantitative comparison of robustness and scanning velocity is presented in Table 1. The lowest

Table 1 Scanning velocity and vibration resulting from 10% modeling error

Parameter	Type of shaped input			
	ZV	ZVD	UM ZV	UM ZVD
Lowest scan velocity, v_1 (cm/s) possible	4.0	6.0	3.6	4.7
Vibration with 10% error (in scan region 4)	4.62	0.80	5.50	1.03

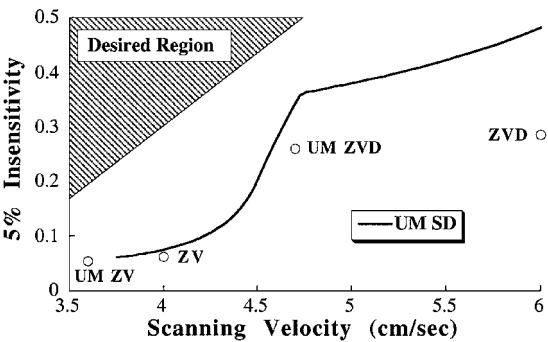


Fig. 6 Insensitivity vs scanning velocity.

scan velocities possible with each shaper are listed along with the vibration that occurs when there is a 10% error in the natural frequency of the system. These values reflect the results from a 0.25 s cycle with a maximum velocity of 19.2 cm/s. The vibration amplitude data was taken from region 4 of the response because that region had the highest amplitude of vibration of the four scan regions. These results clearly illustrate the trade-off that exists among these four shapers.

Figure 6 shows the scanning velocities of each shaper plotted against the 5% insensitivity of the shapers. Shapers that produce a low scanning velocity tend to have relatively low robustness, whereas shapers that produce robust commands tend to require higher scanning velocities. The region on the plot marked "desired region" represents the ideal system response, a low scanning velocity and high robustness. The figure shows that the commonly available shapers discussed thus far allow only four possible combinations of scan velocity and robustness. The following section presents an input shaper design algorithm that allows this trade-off to be set at any desired level.

IV. Specified-Duration Shapers

To approach the desired performance region shown in Fig. 6, an input shaper can be designed using the UM amplitude constraints,¹⁵ setting the shaper duration to a desired value, and maximizing the 5% insensitivity. This process was first suggested for designing input shapers for cranes so that the time lag introduced by shaping could be set to a value that was comfortable to the human operator.¹⁶ Here we expand on the idea by allowing the shaper duration to vary over a wide range. By varying the shaper duration, the trade-off between robustness and the resulting scanning velocity can be clearly understood.

This shaper design method was first implemented using a shaper duration equal to the duration of a ZVD shaper. (This duration is the period of system vibration, T .) Figure 4 compares the sensitivity curve of this shaper, called the UM Specified-Duration (UM SD) shaper, to that of the ZVD shaper. It is clear that the UM SD shaper provides greater robustness for the same duration as the ZVD shaper. In fact, the 5% insensitivity of the UM SD shaper is 0.482, which is significantly more than the 0.286 of the ZVD shaper.

The scanning velocity vs 5% insensitivity for the UM SD shaper is plotted along with the points corresponding to the standard input shapers in Fig. 6. Notice that the gain in robustness provided by the UM SD shaper becomes much larger as the scanning velocity (shaper duration) is increased. The use of this shaper moves the trade-off between robustness and scan velocity closer to the desired region. For example, the insensitivity of a ZVD shaper is 0.286 and the scanning velocity is 6 cm/s. With the UM SD shaper, this same

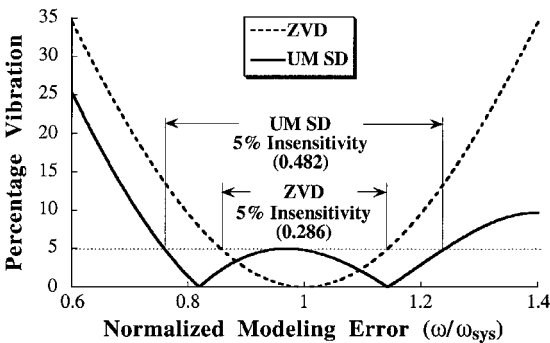


Fig. 4 Sensitivity curves for the ZVD and UM SD shapers.

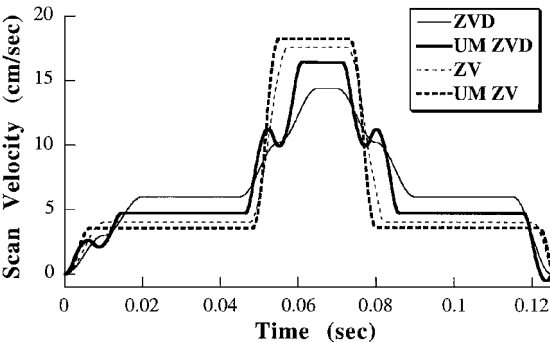


Fig. 5 Velocity responses to several types of shaped inputs.

degree of insensitivity can be achieved with a scan velocity of only 4.61 cm/s. Furthermore, the UM SD design process allows greater flexibility by generating a shaper that produces any desired scan velocity, or, conversely, any desired level of robustness.

The SD shaper contains negative impulses, so it has the possibility of exciting the higher modes of the spacecraft. If, after the dominant low mode has been eliminated by the SD shaper, the higher modes become problematic, then the above design procedure must be augmented with constraints that limit the high-mode vibration. Techniques for doing this are readily available in the literature.^{15,17}

V. Conclusions

It has been shown that input shaping can be used to reduce vibration during constant-velocity scanning with flexible systems. However, the input shaping process increases the cycle time and shortens the regions over which the system travels at constant velocity. A procedure was presented to overcome these drawbacks by modifying the unshaped command before input shaping is implemented. Given cycle-time constraints, the command modification increases the scan velocity. Because this increase is proportional to the duration of the input shaper, a short-duration shaper is necessary to produce a low scan velocity. The duration of a shaper is dependent on its robustness; therefore, increasing the robustness of the input shaping process requires an increase in scan velocity. An input shaper design procedure was developed to optimally balance the trade-off between robustness and scan velocity.

References

1. "An Evaluation of Reaction Wheel Emitted Vibrations for Large Space Telescope," NASA TR N76-18213, Sperry Flight Systems, 1976.
2. Bialke, B., "A Compilation of Reaction Wheel Induced Spacecraft Disturbances," *20th Annual American Astronautical Society Guidance and Control Conference*, AAS Paper 97-038, Feb. 1997, pp. 93–103.
3. Rodden, J. J., Dougherty, H. J., Reschke, L. F., Hasha, M. D., and Davis, L. P., "Line of Sight Performance with Reaction Wheel Isolation," *Proceedings of the Annual Rocky Mountain Guidance and Control Conference*, AAS Paper 86-005, Feb. 1986, pp. 71–84.
4. Liu, Q., and Wie, B., "Robust Time-Optimal Control of Uncertain Flexible Spacecraft," *Journal of Guidance, Control, and Dynamics*, Vol. 15, No. 3, 1992, pp. 597–604.
5. Singh, T., Vadali, S. R., and Abhyankar, N., "Robust Time-Delay Control of Multimode Systems," *American Control Conference*, June 1994.
6. Singhose, W., Bohlke, K., and Seering, W., "Fuel-Efficient Pulse Command Profiles for Flexible Spacecraft," *Journal of Guidance, Control, and Dynamics*, Vol. 19, No. 4, 1996, pp. 954–960.
7. Givoli, D., and Rand, U., "Minimization of Thermoelastic Deformation in Space Structures Undergoing Periodic Motion," *Journal of Spacecraft and Rockets*, Vol. 32, No. 4, 1995, pp. 662–669.
8. Woodard, S., "Orbital and Configuration Influences on Spacecraft Dynamic Response," *Journal of Spacecraft and Rockets*, Vol. 35, No. 2, 1998, pp. 177–182.
9. Hung, R. J., Long, Y. T., and Chi, Y. M., "Slosh Dynamics Coupled with Spacecraft Attitude Dynamics, Part 1: Formulation and Theory," *Journal of Spacecraft and Rockets*, Vol. 33, No. 4, 1996, pp. 575–581.
10. Butterfield, A., and Woodard, S., "Measured Spacecraft Instrument and Structural Interactions," *Journal of Spacecraft and Rockets*, Vol. 33, No. 4, 1996, pp. 556–562.
11. Ellison, J., Ahmadi, G., and Grodinsky, C., "Evaluation of Passive and Active Vibration Control Mechanisms in a Microgravity Environment," *Journal of Spacecraft and Rockets*, Vol. 32, No. 2, 1995, pp. 375–376.
12. Maghami, P. G., Joshi, S. M., and Price, D. B., "Integrated Controls-Structures Design Methodology for Flexible Spacecraft," *Journal of Spacecraft and Rockets*, Vol. 32, No. 5, 1995, pp. 839–844.
13. Singer, N. C., and Seering, W. P., "Preshaping Command Inputs to Reduce System Vibration," *Journal of Dynamic Systems, Measurement, and Control*, Vol. 112, March 1990, pp. 76–82.
14. Smith, O. J. M., *Feedback Control Systems*, McGraw-Hill, New York, 1958.
15. Singhose, W., Singer, N., and Seering, W., "Time-Optimal Negative Input Shapers," *Journal of Dynamic Systems, Measurement, and Control*, Vol. 119, June 1997, pp. 198–205.
16. Singer, N., Singhose, W., and Krikkku, E., "An Input Shaping Controller Enabling Cranes to Move Without Sway," *Proceedings of the ANS 7th Topical Meeting on Robotics and Remote Systems*, May 1997.
17. Singhose, W., and Grosser, K., "Limiting Excitation of Unmodeled High Modes with Negative Input Shapers," *Proceedings of the IEEE Conference on Control Applications*, Aug. 1999.

Worst-Case Distributions for Performance Evaluation of Proportionally Guided Missiles

Keren Rinat* and Joseph Z. Ben-Asher†
Technion—Israel Institute of Technology,
32000 Haifa, Israel

Nomenclature

d	= gyro drift
N'	= proportional navigation gain
n_C	= missile's commanded acceleration
n_M	= missile's acceleration
n_T	= target's acceleration
R_a	= line-of-sight length
t_f	= conflict duration
V_C	= closing velocity
V_M	= missile's velocity
V_T	= target's velocity
γ_M	= missile's path angle
γ_T	= target's path angle
λ	= line-of-sight angle
τ	= missile's time constant

I. Introduction

PERFORMANCE analysis of guided missiles involves uncertain events such as the engagement duration, the type of evasive maneuvers performed by the target, or the end-game environmental conditions. Under certain simplifying assumptions, the analysis can be performed analytically,¹ but more frequently, numerical Monte Carlo simulations are used for the performance analysis. A Monte Carlo simulation is a statistical sampling experiment on a model of the system. Uncertain parameters are treated as stochastic variables and are drawn from a random number generator based on assumed distributions. Each simulation run is performed with a set of sampled variables, and the performance evaluation is based on postanalyzing a large number of simulations.

Recently, Barmish and Lagoa² investigated the problem of finding probability distributions that yield worst-case performance for general systems. Under some fairly mild assumptions, namely, 1) zero mean random variables (RV), 2) known support intervals, that is, ranges of change for the various RV, and 3) the probability density functions (PDF) are symmetrical and nonincreasing with respect to the absolute value of the RV, the worst-case distributions can be represented by truncated uniform distributions. A truncated uniform distribution is a uniform (rectangular) distribution defined over a subinterval of the original support interval. This is a very important result because it transforms the problem from infinite- to finite-dimensional space. Thus, for each random variable, a single parameter, namely, the width of its associated subinterval, characterizes the worst-case distribution. These parameters are to be searched for, to evaluate the worst-case performance of the system.

The purpose of the present research is to apply this result to the field of missile guidance. As already said, several uncertain parameters are always involved in the performance evaluation of guided missiles. To search for the worst-case distributions seems to be a viable approach, as opposed to arbitrarily assuming fixed PDF. To this end we focus here on proportionally guided missiles with the engagement duration as a single stochastic variable. Reference 3 extends the results to include stochastic evasive maneuvers in addition to the end-game duration, an extension that requires more advanced numerical optimization techniques. However, even in the

Received 10 September 1999; revision received 5 January 2000; accepted for publication 15 April 2000. Copyright © 2000 by the American Institute of Aeronautics and Astronautics, Inc. All rights reserved.

*Graduate Student, Department of Aerospace Engineering.

†Associate Professor, Department of Aerospace Engineering. Senior Member AIAA.